

An “All-Green” Catalytic Cycle of Aqueous Photoionization

Martin Goez,* Christoph Kerzig, and Robert Naumann

Abstract: Hydrated electrons are highly aggressive species that can force chemical transformations of otherwise unreactive molecules such as the reductive detoxification of halogenated organic compounds. We present the first example of the sustainable production of hydrated electrons through a homogeneous catalytic cycle driven entirely by green light (532 nm, coinciding with the maximum of the terrestrial solar spectrum). The catalyst is a metal complex serving as a “container” for a radical anion. This active center is generated from a ligand through quenching by a sacrificial electron donor, is shielded by the complex such that it stores the energy of the photon for much longer than a free radical anion could, and is finally ionized by another photon to regenerate the ligand and recover the starting complex quantitatively. The sacrificial donor can be a bioavailable reagent such as ascorbic acid.

At least two green photons are needed for the production of one hydrated electron e_{aq}^- from stable source molecules, because the photon energy (2.33 eV at 532 nm) is only about 80 to 90 % of the standard potential of e_{aq}^- (2.77 V against the normal hydrogen electrode, NHE).^[1] Having in mind the ultimate aim of utilizing the sun as the (low-flux) light source, it is the most promising strategy to employ two successive single-photon absorptions and store the energy of the first photon in an intermediate. Examples of electron detachment by green light are known for all common classes of photochemical intermediates, excited singlet states,^[2] triplet states,^[3,4] radicals,^[5–7] and radical anions,^[8–12] but the longer such an intermediate lives, the more likely it is to absorb the ionizing second photon. This suggests that the usefulness for this process increases in the order excited singlet (ns) < triplet (μs) < radical or radical anion (no photophysical deactivation).

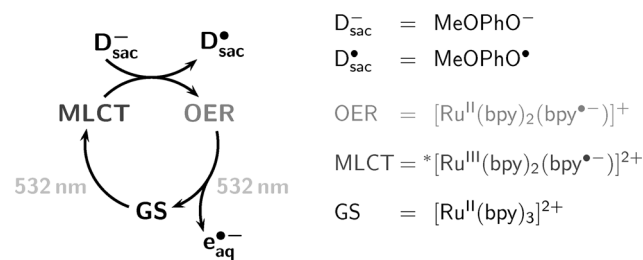
As recently advocated by us,^[12] the radical anion $A^{\bullet-}$ appears inherently better suited for the sustainable generation of e_{aq}^- than the other intermediates on yet other grounds. The gentlest and most natural way to prepare a substrate A for its ionization is the addition of one loosely bound extra electron to it in the first place, which is easily achieved by photoinduced electron transfer from a sacrificial donor to excited A. The ionization of $A^{\bullet-}$ is assisted by the formation of a stable molecule as the by-product, namely the starting material A. By the same token, a two-photon ionization via the radical anion constitutes a catalytic cycle in which the photons switch the catalyst between its light-absorbing forms

A and $A^{\bullet-}$. An optimization of the overall reaction is greatly facilitated by the divergent roles of the two components. As long as the sacrificial donor quenches the excited catalyst efficiently enough and does not unduly absorb itself, the price and availability are the most important selection criteria for that expendable item, whereas the catalyst can be tailored for optimum photophysical and photochemical properties of its different forms without an expensive and/or difficult synthesis being prohibitive.

In the present work, the bipyridine radical anion functions as the electron precursor, and we have extended its life greatly by using the one-electron-reduced form OER of the extremely popular sensitizer ruthenium (tris)bipyridine^[13] as its “container”. We prepare OER by reductive quenching of the green-light-excited complex with 4-methoxy phenolate D_{sac}^- .^[14] Not only does OER contain a localized bipyridine radical anion with a strong $\pi-\pi^*$ absorption in the green,^[15] but it is also stable for seconds in deaerated aqueous solution,^[16] except for bimolecular termination with the quencher-derived radical D_{sac}^\bullet . This contrasts very favorably with the fate of the free radical anion, which is protonated on a sub-nanosecond timescale even at pH 14 and then undergoes diffusion-controlled disproportionation.^[17] As we will show, another green photon ionizes OER and regenerates the starting complex without any side reactions that would destroy the catalyst.

Our investigation method is nanosecond laser-flash photolysis with two superimposed, independently triggered 532 nm beams (for experimental details see Section S1 in the Supporting Information). The catalytic cycle is displayed in Scheme 1, which also contains the formulas of all species involved. Our experiments for establishing the mechanism are summarized in Figure 1. The numbering of the following list is identical with the numbering of the figure’s subgraphs; for full particulars, we refer to the pertaining Sections S2–S5.

1 a) A first green photon excites the ground state (GS) of the complex, producing the metal-to-ligand charge-transfer excited state MLCT quantitatively and fully reversibly; MLCT is photochemically inert in the green.



Scheme 1. Photoionization mechanism and formulas of all species involved.

[*] Prof. Dr. M. Goez, C. Kerzig, R. Naumann
Martin-Luther-Universität Halle-Wittenberg, Institut für Chemie
Kurt-Mothes-Str. 2, 06120 Halle/Saale (Germany)
E-mail: martin.goez@chemie.uni-halle.de



Supporting information for this article is available on the WWW under <http://dx.doi.org/10.1002/ange.201405693>.

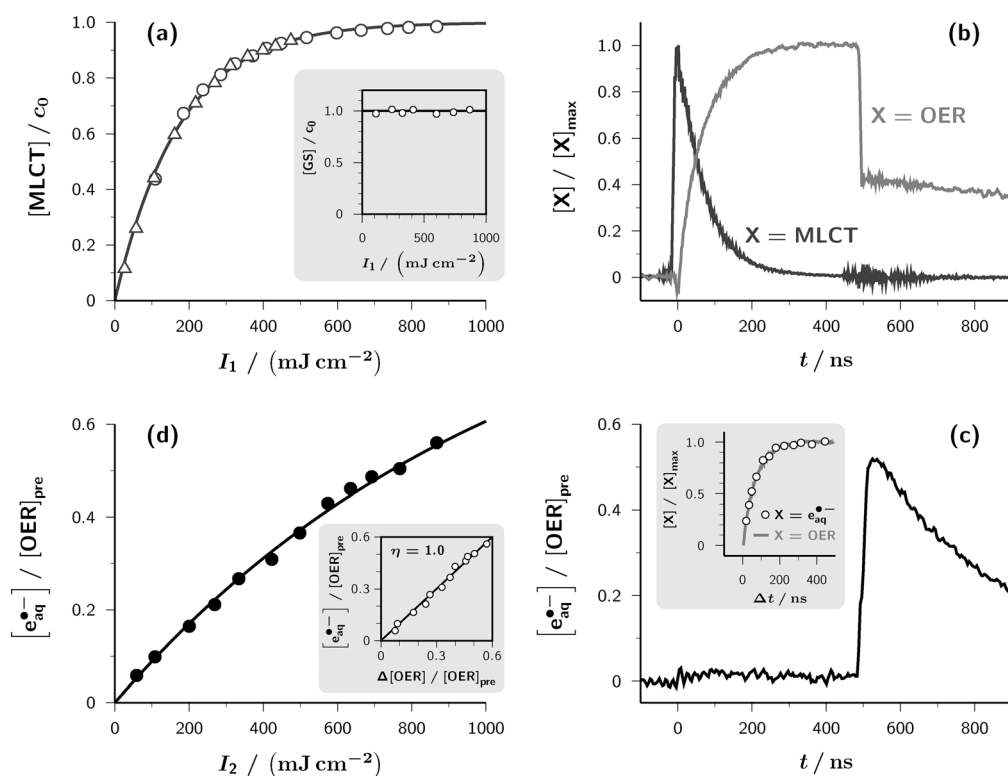


Figure 1. Laser-flash (532 nm) photolysis results for the system ruthenium (tris)bipyridine/4-methoxyphenolate (GS/ D_{sac}^-). Experimental conditions unless specifically noted: aqueous solution of $5 \times 10^{-5} M$ GS and $2.5 mM$ D_{sac}^- at pH 12.7; first laser flash, 0 ns, $410 mJ cm^{-2}$; second laser flash, 500 ns, $867 mJ cm^{-2}$. a) Experiments in the absence of D_{sac}^- . Main plot: MLCT concentration relative to substrate concentration c_0 as a function of the excitation intensity I_1 , single-flash experiments with first (triangles) or second (circles) laser only; the solid curve is the best-fit function $1 - \exp[-I_1 / (174 mJ cm^{-2})]$. Inset: two-flash experiments with excitation by the stronger laser at variable intensity I_1 , waiting for complete decay of MLCT, and then probing the complex concentration with the weaker laser at constant intensity; the solid line is the normalized ground-state concentration with the first flash omitted. b) Normalized traces for the MLCT (dark gray) and OER (gray) concentrations obtained with the separation explained in detail in Section S4 of the Supporting Information. The oscillations between 450 and 700 ns are due to the constructive interference of Q-switch pickup from both lasers. c) Main plot: trace of the $e_{aq}^{\bullet-}$ concentration (for details, see Section S5 of the Supporting Information) relative to the concentration of OER before the second laser flash, $[OER]_{pre}$, obtained under the same conditions as the traces of the preceding subgraph. Inset: normalized OER concentration rise (gray trace) following the first laser flash and $e_{aq}^{\bullet-}$ concentration (black circles) obtained after the second laser flash as functions of the interpulse delay Δt . d) Main plot: $e_{aq}^{\bullet-}$ concentration relative to $[OER]_{pre}$ as a function of the intensity I_2 of the second laser flash, with the best-fit function (solid curve) given by $1 - \exp[-I_2 / (1072 mJ cm^{-2})]$; inset, same relative $e_{aq}^{\bullet-}$ concentration as a function of the relative OER bleaching, slope of the regression line, 1.002, zero intercept. For further explanations, see the text.

Of the species present at the start of the experiment, only GS absorbs at 532 nm (compare Section S2). Intersystem crossing of the primarily formed locally excited complex to give MLCT occurs on a sub-picosecond timescale and quantitatively.^[13] As the main plot of Figure 1a shows, the intensity dependence of MLCT formation is given by a saturation curve, and more than 90% of GS can be converted to MLCT within the flash duration even with the weaker of our two lasers. Unquenched MLCT reverts to the GS without side reactions, accompanied by an emission that allows its quantitative monitoring.^[13] MLCT absorbs weakly at 532 nm (see Section S2), but the resulting higher excited state *MLCT is short-lived on the timescale of our laser flashes, and this further excitation does not lead to the decomposition of the complex and specifically not to ionization.^[18] The inset of Figure 1a demonstrates this chemical stability of both MLCT and

*MLCT: Producing variable amounts of MLCT and *MLCT with a first flash, then allowing them to deactivate completely, and then probing the concentration of GS with a second flash of constant intensity gives the same result regardless of the intensity of the first flash.

1b) Reductive quenching of MLCT by the sacrificial donor D_{sac}^- yields OER, which is then bleached by a second green photon.

By choosing the quencher concentration as explained in Section S3, we were able to create a situation in which there is hardly any quenching ($< 4\%$) during each laser flash but largely complete quenching ($> 86\%$) during the waiting period between the flashes, meaning that the light-driven and thermal reaction steps are temporally separated. Most of the quenching events are chemically non-productive, however, and with 4-methoxy phenolate we found an efficiency η of only 0.18 for persistent OER formation after MLCT quenching.

We observed MLCT and OER under conditions, in which there is no cross-dependence of their

signals and no other species interfere with their detection (see Section S3). Their time evolution up to the start of the second laser pulse is displayed in Figure 1b, but this pulse acts on both the newly generated OER and the much greater amount of GS still present, therefore the contribution of the latter to the observables must be removed. This can be effected quantitatively and reliably by the separation described in Section S4, which gave the curves displayed in the later part of Figure 1b (from 500 ns onwards). The procedure filters out the traces of a hypothetical experiment with complete conversion of the GS into OER during the interpulse delay and no new production of MLCT by the second laser. As is clearly observed, it isolates a bleaching of OER by the second laser pulse, which proves that upon 532 nm excitation OER undergoes a photoreaction.

1c) The second photon liberates $e_{\text{aq}}^{\bullet-}$ in proportion to the amount of OER present.

To capture only $e_{\text{aq}}^{\bullet-}$, we performed different experiments with and without the electron scavenger N_2O (see Section S5), an established method in radiation chemistry.^[1] The main plot of Figure 1c displays the outcome at the same reactant concentration, laser intensity, and timing as in Figure 1b. In striking contrast, the first laser pulse yields practically no $e_{\text{aq}}^{\bullet-}$, whereas the second produces a large amount. Reversing the order of the two pulses identifies that as an effect unrelated to the different laser powers. Instead, there is a strict proportionality between the concentration of OER at the moment before the second laser flash and the concentration of $e_{\text{aq}}^{\bullet-}$ produced by this laser flash. This can be demonstrated by varying the interpulse delay, as shown in the inset of Figure 1c, or by varying the intensity of the first laser pulse. Because the stoichiometrically formed quenching product $\text{D}_{\text{sc}}^{\bullet}$ is not ionizable with green light (see Section S2), these findings pinpoint OER as the source of $e_{\text{aq}}^{\bullet-}$. The minute amount of $e_{\text{aq}}^{\bullet-}$ generated by the first pulse can be traced to the small quantity of OER already formed during that pulse.

1d) OER bleaching and $e_{\text{aq}}^{\bullet-}$ formation are monophotonic processes with identical quantum yields; autoionization is the only chemical deactivation pathway of the green-light-excited OER.

Figure 1d displays the electron yield relative to the prepulse concentration of OER as a function of the laser intensity (in the main plot) and against the relative bleaching of OER (in the inset). The linear low-intensity regime of the saturation curve in the former graph, with successful straight-line extrapolation to the origin of the coordinate system,^[19] characterizes the green-light ionization of OER as monophotonic; the unit slope in the latter graph reveals that one $e_{\text{aq}}^{\bullet-}$ is produced per OER molecule bleached.

Taking the ratio of the best-fit constants κ in Figure 1d and Figure 1a, each of which is proportional to the quantum yield of the respective process and the extinction coefficient of the species absorbing the photon,^[12] we found a quantum yield of 0.013 for the photoionization of OER with 532 nm. This approach employs GS as an inner actinometry standard, so very effectively cancels uncertainties of the absolute excitation intensities and homogeneity. By redetermining the extinction coefficient of OER relative to that of $e_{\text{aq}}^{\bullet-}$ (see Section S2), we also eliminated errors related to that quantity.

To optimize the overall performance, we tested the ascorbate dianion as a bioavailable replacement for the phenolate, both in aqueous solution and in SDS (sodium dodecyl sulfate) micelles. Although a very popular reductive quencher of MLCT,^[20] ascorbic acid was hitherto employed only as the neutral acid or the monoanion. We found that the dianion quenches much faster (7.6×10^9 and $3.9 \times 10^7 \text{ M}^{-1} \text{ s}^{-1}$ in water and in the micelles). More importantly, the efficiency η of the OER formation after the primary electron transfer is twice as high (0.38, regardless of the medium) as that of the phenolate. Also, the compartmentalization by the micelle strongly suppresses the recombination of OER with the

quencher-derived radical such that the life of OER becomes longer than milliseconds.

The only other green-light photoionization of stable molecules in solution known to date is that of perylene-3-amine,^[21] which is mechanistically controversial (see Section S6) and consumes a substrate that is expensive to prepare. The example we have presented here is the very first case of such an “all-green” photoionization through a catalytic cycle. It consumes only cheap and even bioavailable reagents and might thus have the potential to be developed into a sustainable source of $e_{\text{aq}}^{\bullet-}$ for chemical applications such as the reductive detoxification of organic waste with sunlight, which up to now has only been achieved radiolytically^[22] or with UVC radiation.^[23]

Received: May 27, 2014

Published online: July 22, 2014

Keywords: green chemistry · photocatalysis · photoionization · radical ions · sustainable chemistry

- [1] J. W. T. Spinks, R. J. Woods, *An Introduction to Radiation Chemistry*, 2. ed., Wiley, New York, 1976.
- [2] M. Hara, S. Samori, X. Cai, M. Fujitsuka, T. Majima, *J. Phys. Chem. A* **2005**, *109*, 9831–9835.
- [3] Z. Wang, W. G. McGimpsey, *J. Phys. Chem.* **1993**, *97*, 9668–9672.
- [4] L. J. Johnston, R. W. Redmond, *J. Phys. Chem. A* **1997**, *101*, 4660–4665.
- [5] R. W. Redmond, J. C. Scaiano, L. J. Johnston, *J. Am. Chem. Soc.* **1990**, *112*, 398–402.
- [6] M. Sakamoto, X. Cai, S. S. Kim, M. Fujitsuka, T. Majima, *J. Phys. Chem. A* **2007**, *111*, 223–229.
- [7] M. Goez, C. Kerzig, *Angew. Chem.* **2012**, *124*, 12775–12777; *Angew. Chem. Int. Ed.* **2012**, *51*, 12606–12608.
- [8] U. Sowada, R. A. Holroyd, *J. Phys. Chem.* **1981**, *85*, 541–547.
- [9] P. Natarajan, R. W. Fessenden, *J. Phys. Chem.* **1989**, *93*, 6095–6100.
- [10] T. Majima, M. Fukui, A. Ishida, S. Takamuku, *J. Phys. Chem.* **1996**, *100*, 8913–8919.
- [11] J.-C. Gummy, E. Vauthey, *J. Phys. Chem. A* **1997**, *101*, 8575–8580.
- [12] M. Goez, B. H. M. Hussein, *Phys. Chem. Chem. Phys.* **2004**, *6*, 5490–5497.
- [13] S. Campagna, F. Puntoriero, F. Nastasi, G. Bergamini, V. Balzani, *Top. Curr. Chem.* **2007**, *280*, 117–214.
- [14] K. Miedlar, P. K. Das, *J. Am. Chem. Soc.* **1982**, *104*, 7462–7469.
- [15] P. S. Braterman, A. Harriman, G. A. Heath, L. J. Yellowlees, *J. Chem. Soc. Dalton Trans.* **1983**, 1801–1803.
- [16] Q. G. Mulazzani, S. Emmi, P. G. Fuoichi, M. Z. Hoffman, M. Venturi, *J. Am. Chem. Soc.* **1978**, *100*, 981–983.
- [17] Q. G. Mulazzani, S. Emmi, P. G. Fuoichi, M. Venturi, M. Z. Hoffman, M. G. Simic, *J. Phys. Chem.* **1979**, *83*, 1582–1590.
- [18] M. Goez, D. von Ramin-Marro, M. H. O. Musa, M. Schiewek, *J. Phys. Chem. A* **2004**, *108*, 1090–1100.
- [19] U. Lachish, A. Shafferman, G. Stein, *J. Chem. Phys.* **1976**, *64*, 4205–4211.
- [20] B. Shan, T. Baine, X. A. N. Ma, X. Zhao, R. H. Schmehl, *Inorg. Chem.* **2013**, *52*, 4853–4859.
- [21] J. K. Thomas, P. Piciulo, *J. Am. Chem. Soc.* **1978**, *100*, 3239–3240.
- [22] Y. Peng, S. He, J. Wang, W. Gong, *Radiat. Phys. Chem.* **2012**, *81*, 1629–1633.
- [23] X. Li, J. Ma, G. Liu, J. Fang, S. Yue, Y. Guan, L. Chen, X. Liu, *Environ. Sci. Technol.* **2012**, *46*, 7342–7349.